

Numerical simulation of recent shrinkage of Khumbu Glacier, Nepal Himalayas

NOZOMU NAITO, MASAYOSHI NAKAWO

*Institute for Hydrospheric-Atmospheric Sciences, Nagoya University, Furo-cho, Chikusa-ku,
Nagoya 464-8601, Japan*

e-mail: naito@ihas.nagoya-u.ac.jp

TSUTOMU KADOTA

*Frontier Observational Research System for Global Change, Sumitomo Hamamatsu-cho
Building 4F, 1-8-16 Hamamatsu-cho, Minato-ku, Tokyo 105-0013, Japan*

CHARLES F. RAYMOND

*Geophysics Program, University of Washington, Box 351650, Seattle, Washington 98195-1650,
USA*

Abstract A new model for coupled mass balance and flow of a debris-covered glacier was developed to account for the effects of supraglacial debris on glacier evolution. The model is reasonably consistent with observations of recent shrinkage of the ablation area of Khumbu Glacier, Nepal Himalayas from 1978 to 1999. The model predicts formation and succeeding enlargement of a depression in the lower ablation area. This depression could result in the formation of a glacial lake. Potential improvements to the model for a debris-covered glacier are identified.

INTRODUCTION

The ablation areas of most large glaciers in the Himalayas are covered with thick supraglacial debris. It is, hence, important to know how these debris-covered glaciers in the Himalayas respond to climate change in order to predict consequences for local water resources and sea level rise.

Khumbu Glacier is one of the largest debris-covered glaciers in the Nepal Himalayas. It flows down from the slopes of Mts Everest (8848 m, Sagarmatha or Qomolangma), Lhotse (8511 m) and Nuptse (7861 m) (Fig. 1). Its total length is more than 15 km and its present terminus is located at about 4900 m a.s.l. The accumulation area, called the West Cwm, is nearly inaccessible due to an ice fall. The equilibrium line altitude (ELA) is located in this ice fall at about 5600 m a.s.l. More glaciological research has been undertaken on the ablation area than on any other debris-covered glacier in the Himalayas. Recent thinning of the glacier has been measured (Kadota *et al.*, 2000). This study establishes a new numerical model to simulate the recent shrinkage of the glacier accounting for supraglacial debris and its effects on ablation.

MODEL DESCRIPTION

The continuity equation coupling mass balance and glacier flow was formulated using the finite-volume method (Patankar, 1980; Lam & Dowdeswell, 1996):

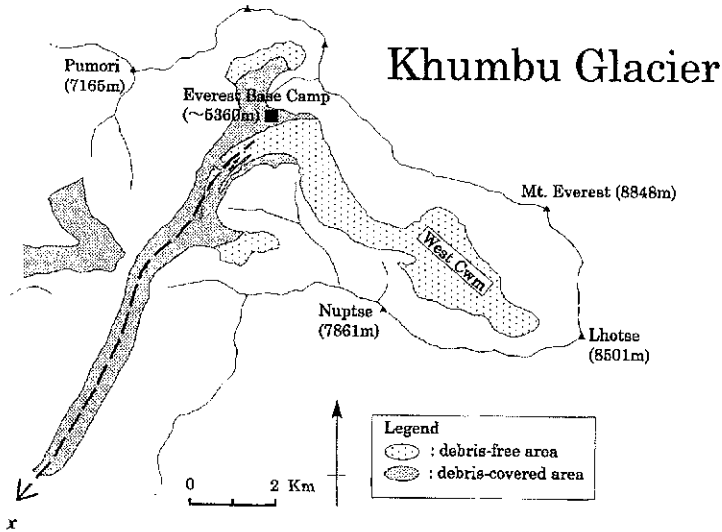


Fig. 1 Illustrated map of Khumbu Glacier. The study area is along a central flow line indicated as a dashed line with an arrow.

$$\frac{\Delta V}{\Delta t} = b\bar{W}\Delta x - (Q_{out} - Q_{in}) \quad (1)$$

where V , b , \bar{W} and Q represent volume between fixed vertical cross-sections, mass balance rate, glacier surface width averaged between the sections, flux through the boundary cross-section to/from neighbouring control-volumes, respectively. Subscripts for Q refer to outgoing or incoming flux, t and x are time and horizontal distance along a flow line traced in Fig. 1. Time step, Δt , was 1/36 year (about 10 days), and the longitudinal length of each control-volume (grid space), Δx , was 500 m. Equation (1) was stepped forward in time using an implicit Crank-Nicholson scheme with calculations of mass balance and glacier flow described in the following subsections. The simulation, however, was limited to the ablation area with an assumption about flux through the upper boundary cross-section, which will be described later. A trapezoidal cross-section was assumed for the glacier channel with lateral slopes of 40° and 35° for the right and left bank sides, respectively, as compatible with a topographic survey by Glaciological Expedition of Nepal (1980). Glacier width was approximated with a linear variation to fit measurements from the topographic map published by the National Geographic Society (1988). The profile of the glacier bed was determined by ice thickness measurements with ice penetrating radar (Gades *et al.*, 2000) and topographic surveys in 1999.

Mass balance

Glaciers in the Himalayas are fed mostly in summer, and this summer-accumulation-type mass balance has to be taken into consideration. Empirical equations among air temperature T ($^\circ\text{C}$), precipitation rate P (m day^{-1}), accumulation rate c (m day^{-1}) and ablation rate a (m day^{-1}) were obtained for a debris-free glacier in the Nepal Himalayas by Ageta (1983) and Ageta & Kadota (1992) as follows:

$$\begin{aligned}
 c &= P && \text{when } T < -0.6 \\
 &= P(0.85 - 0.24T) && \text{when } -0.6 \leq T \leq 3.5 \\
 &= 0 && \text{when } T > 3.5 \\
 a &= 0 && \text{when } T < -3.0 \\
 &= -0.0001(T + 3.0)^{3.2} && \text{when } -3.0 \leq T \leq 2.0 \\
 &= -0.009T && \text{when } T > 2.0
 \end{aligned} \tag{2}$$

Seasonal variations in P and T were approximated by sinusoidal variations, having the same phase (i.e. high/low in summer/winter). Annual mean air temperature was set to be compatible with a measurement in 1973–1974 at Lhajung (0.5°C at 4420 m a.s.l.) (Inoue, 1976), accounting for a fixed altitudinal lapse rate of $-6 \times 10^{-3} \text{ }^\circ\text{C m}^{-1}$. Annual range of air temperature and annual precipitation were assumed to be the same as at Lhajung (15°C and 540 mm, respectively) and independent of altitude. Lhajung is located at about 5 km southeast of the Khumbu Glacier terminus.

Effects of debris cover on the ablation have been examined in the following ways. Nakawo *et al.* (1999) estimated the longitudinal distribution of the ablation rate for the whole ablation area, using satellite data and meteorological data. As accumulation to the glacier ice body is negligible on the debris-covered ablation area, the estimated ablation rate was taken to be equivalent to the mass balance rate. They, however, implied that the magnitude of the mass balance rate may be in error due to uncertainty in meteorological data input. Surface lowering rate calculated by the continuity equation with observed surface flow speed was compared with that measured by Kadota *et al.* (2000). The comparison indicated that the calculated surface lowering rate was larger than the measurement on the lowest part of the glacier. The longitudinal distribution of mass balance rate, therefore, was slightly modified from the estimate by Nakawo *et al.* (1999) as shown in Fig. 2(a). A hypothetical mass balance rate for debris-free conditions is also shown in Fig. 2(a), which was calculated with equation (2) with the distribution and the seasonal variation of air temperature based on the surface altitude from the topographic surveys in 1978 (Watanabe *et al.*, 1980). The ratio r of the mass balance for debris-covered conditions to that for debris-free conditions was evaluated from the solid and dashed curves in Fig. 2(a). The longitudinal distribution of debris thickness H_d was measured by Nakawo *et al.* (1986) and Watanabe *et al.* (1986). The implied relationship between r and H_d is shown in Fig. 2(b).

As a result, net ablation (negative mass balance) on the debris-covered area can be calculated from c , a in equation (2) and r which depends on H_d (Fig. 2(b)). However, special attention must be given to the situation when supraglacial debris is covered with snow. If debris cover is buried by snow cover, water equivalent thickness of the snow cover H_s varies depending on $c + a$ in equation (2), and the mass of glacier ice beneath the debris cover does not change. There is no melt-out debris supply from glacier ice in this case. If net ablation exceeds an amount required to melt all the snow cover, however, extra ablation of glacier ice occurs according to the residual amount of net ablation, $(c + a)\Delta t + H_s$ (<0), and the ratio r in Fig. 2(b). Additional debris is, then, supplied as melt-out from the glacier ice. Then, the mass balance rate for glacier ice b is described as:

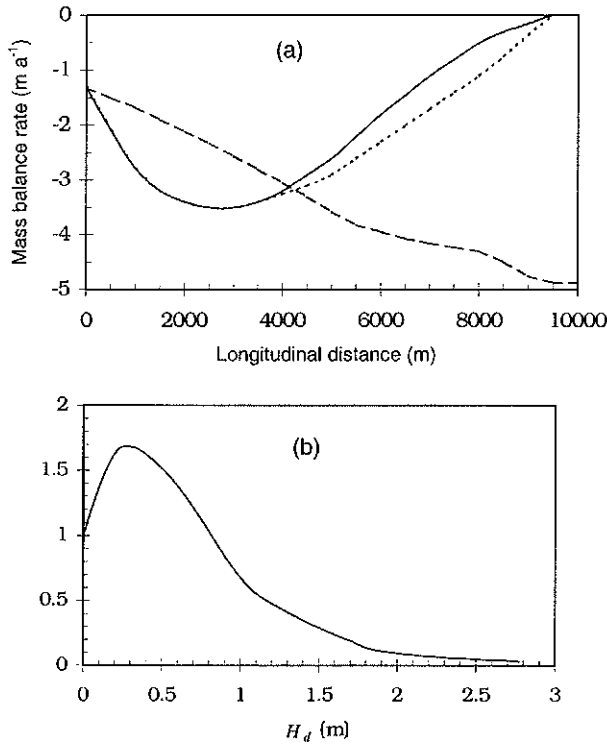


Fig. 2 (a) The mass balance rates on the ablation area of the Khumbu Glacier (dotted line) estimated by Nakawo *et al.* (1999) and (solid line) modified for this simulation with (dashed line) hypothesized for debris-free conditions. (b) The relation between debris thickness H_d and the ratio of mass balance on the debris-covered area to that for debris-free conditions r .

$$\begin{aligned}
 b &= c + a && \text{when } H_d = 0 \\
 &= \frac{r[(c + a)\Delta t + H_s]}{\Delta t} && \text{when } H_d > 0 \text{ and } (c + a)\Delta t + H_s < 0 \\
 &= 0 && \text{when } H_d > 0 \text{ and } (c + a)\Delta t + H_s \geq 0
 \end{aligned} \tag{3}$$

Water equivalent thickness of snow cover H_s varies as:

$$\begin{aligned}
 \frac{\Delta H_s}{\Delta t} &= c + a && \text{when } H_d > 0 \text{ and } (c + a)\Delta t + H_s \geq 0 \\
 H_s &= 0 && \text{in the other cases}
 \end{aligned} \tag{4}$$

Debris thickness H_d varies according to the continuity equation for supraglacial debris:

$$\begin{aligned}
 \frac{\Delta H_d}{\Delta t} &= \frac{C_d}{\rho_d}(-b) - \frac{D_{out} - D_{in}}{W\Delta x} && \text{when } b < 0 \\
 &= -\frac{D_{out} - D_{in}}{W\Delta x} && \text{when } b \geq 0
 \end{aligned} \tag{5}$$

where C_d , ρ_d and D are concentration of debris in glacier ice, density of debris, and flux of supraglacial debris through a boundary between neighbouring control-volume, respectively. The concentration of debris C_d and the density ρ_d were assumed to be constants 0.1 kg m^{-3} and 1220 kg m^{-3} (Nakawo *et al.*, 1986), respectively. Subscripts for D refer to outgoing or incoming flux. The flux D is described as:

$$D = H_d \overline{WU}_s \quad (6)$$

where U_s is surface flow speed, which is described by equation (7) in the next subsection. Note, here, each variable on the right side in equation (6) should be that at the boundary between control-volumes.

Glacier flow

Surface flow speed U_s and flux of glacier ice through a cross-section Q can be described as:

$$U_s = U_d + U_b \quad (7)$$

$$Q = (f_2 U_d + U_b) S \quad (8)$$

$$U_d = \frac{2A}{n+1} (-f_1 \rho g \sin \alpha)^n H^{n+1} \quad (9)$$

U_d is a contribution of ice deformation to the surface flow speed. U_b represents a basal sliding. A and n ($= 3$) are parameters in the flow law of ice; ρ and g are the density of ice and the gravitational acceleration; α , H and S are the surface slope, the central ice thickness and the transversal cross-section area, respectively. f_1 and f_2 are so-called "shape factors", which account for lateral drag in equation (9) and ratio of cross-sectional average ice deformation to U_d in equation (8).

The value of A was assumed to be constant, $6.8 \times 10^{-15} \text{ s}^{-1} (\text{kPa})^{-3}$, which is a recommended value for ice temperature of 0°C by Paterson (1994). The value of the shape factor f_1 was approximated with

$$f_1 = 1 - \frac{0.33^{w/2H} + 0.78^{w/2H}}{2} \quad (10)$$

which fits with the values obtained by Nye (1965) for a parabolic cross-section, as the value of f_1 should not be so different from that for a trapezoidal cross-section, which was used in this model. The flow speed ratio f_2 was assumed to be the same as for laminar flow, $n + 1/n + 2$ ($= 0.8$), which neglects variation in flow speed ratio across the flow. Then U_b was assumed to be distributed in the ablation area independent of time as shown in Fig. 3, which gives surface flow speed U_s consistent with observation (Kodama & Mae, 1976; Nakawo *et al.*, 1999). Inflow from the upper glacier area $Q_m(x=0)$ was assumed to be constant as $5.6 \times 10^9 \text{ kg year}^{-1}$. This value yields agreement between modelled and observed (Kadota *et al.*, 2000) surface lowering at $x=0$, and is about 1.5 times that of an earlier rough estimate by Inoue (1977), which was based on the assumptions that precipitation on the accumulation area would be the same as at Lhajung independent of altitude and that the accumulation area was in a steady state.

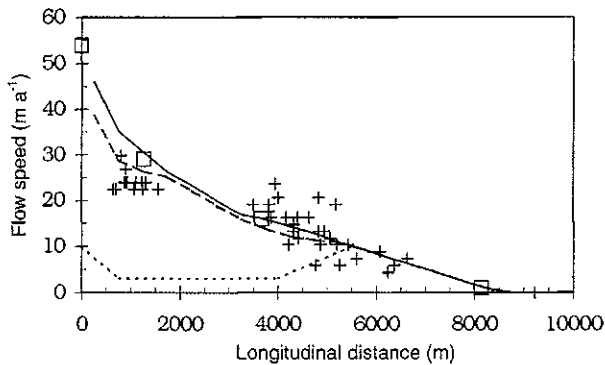


Fig. 3 Flow speeds on the Khumbu Glacier. Square and plus symbols are the observed surface speeds by Kodama & Mae (1976) in 1973–1974 and Nakawo *et al.* (1999) in 1987–1993, respectively. The solid curve represents the calculated surface speed based on the surveyed profile in 1978, and the dashed curve shows that based on a profile in 1990 estimated from topographic surveys in 1978 and 1999. Dotted curve is basal sliding U_b assumed in this study to tune the calculated surface speeds to the observations.

RESULTS OF SIMULATION

The initial conditions were the longitudinal profiles in 1978 of surface elevation (Watanabe *et al.*, 1980) and supraglacial debris thickness (Nakawo *et al.*, 1986; Watanabe *et al.*, 1986). Climate was assumed to be constant as in 1973–1974 (Inoue, 1976), since there are no available data about climate changes around the Khumbu Glacier. Furthermore, Kadota & Ageta (1992) succeeded in simulating shrinkage of a debris-free glacier near the Khumbu Glacier in 1978–1989 without significant climate change, which supports this assumption. Predictions for changes in surface elevation and debris thickness are shown in Fig. 4.

The longitudinal surface profile in 1999 is simulated quite reasonably (Fig. 4(a)). The succeeding simulation predicts that a depression would be formed at about $x = 5.5$ km around year 2020 and the ablation area would be divided into two parts around year 2040. Debris thickness H_d is predicted to decrease on the uppermost part, to increase on the lowest part and near the predicted terminus after the glacier division (Fig. 4(b)).

Sensitivity tests

Sensitivity tests for the simulation of the longitudinal surface profile were examined concerning three important parameters: incoming flux at the upper boundary, basal sliding, and the effect of debris on the mass balance. Figure 5 shows the simulated profiles for 1999 under three different conditions, together with the preceding result. Assuming the incoming flux $Q_{in}(x=0) = 3.8 \times 10^9$ kg year⁻¹ to be the same as Inoue's (1977) earlier rough estimate, the simulated glacier surface lowering during 1978–1999 was predicted to be about twice as large as the observation on the uppermost part. On the other hand, neglecting basal sliding U_b resulted in almost the same surface

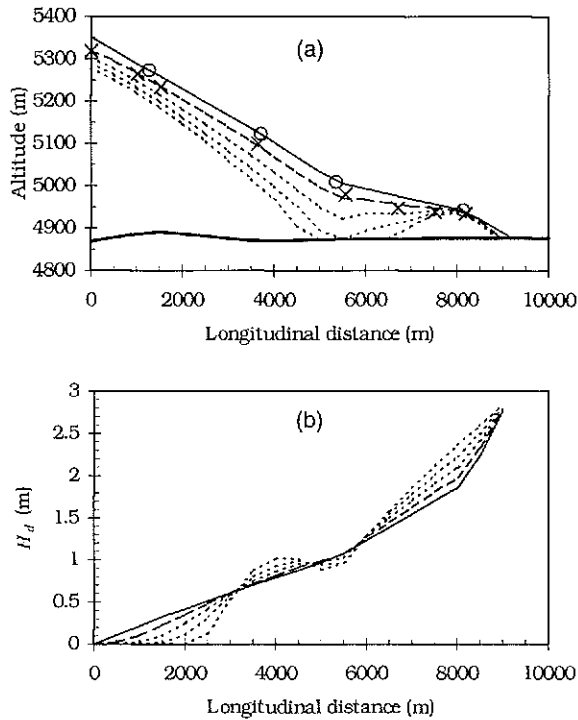


Fig. 4 The results of simulation from 1978. (a) Longitudinal profiles of glacier surface. (b) Longitudinal distributions of debris thickness.

Solid curves mean the initial profile and distribution in 1978. Dashed curves represent simulated results for 1999. Dotted curves are those for 2020, 2040 and 2060. A thick solid line, circle and cross symbols in (a) show the bed profile, and the surface positions estimated from the topographical surveys in 1978 and 1999, respectively.

lowering, although showing a slightly greater lowering on the lower part. Ignoring the effects of supraglacial debris on the mass balance, in other words calculating mass balance everywhere under debris-free conditions only with equation (2), the lowest part was simulated to disappear by 1999.

DISCUSSION

Surface topography of the debris-covered area is so heterogeneous (Iwata *et al.*, 1980) that it is difficult to determine a unique debris thickness depending on x . The debris thickness H_d used in this study should be just an indicator that represents an area average. It must be distinguished from a point debris thickness. The effect of point thickness on ablation has been examined extensively (e.g. Østrem, 1959; Mattson *et al.*, 1993), which shows that debris cover accelerates ablation most effectively at a thickness of a few centimetres, and suppresses it at greater thickness. The relation in this study between the thickness H_d and the mass balance ratio r shown in Fig. 2(b) gives a similar result, although the magnitude of the ratio is different. The present model takes the interaction between the debris thickness and the mass balance into

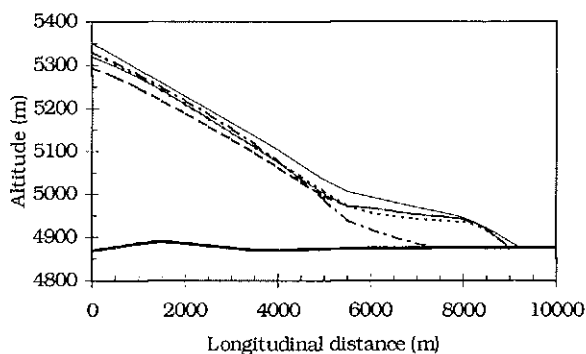


Fig. 5 The results of sensitivity tests for the longitudinal surface profile simulation during 1978–1999. A dashed curve is for $Q_{in}(x=0) = 3.8 \times 10^9 \text{ kg year}^{-1}$ (Inoue, 1977), a dotted curve is for no basal sliding, and a chain curve is for debris-free conditions. The three curves represent simulation results for 1999. The initial profile in 1978 and the original simulation result in 1999 are also shown as in Fig. 4(a) with thin solid curves.

account in a very simplified way through debris conservation (equation (5)) and effects of debris thickness on mass balance (Fig. 2(b)). Without the effects of debris cover on mass balance, actual surface lowering of the glacier especially on the lowest part cannot be simulated as shown by the chain curve in Fig. 5.

Ice cliffs and supraglacial ponds accelerate ablation on the debris-covered area significantly (Inoue & Yoshida, 1980). The mass balance ratio r in Fig. 2(b) includes these effects, because it was based on an ablation rate estimated by Nakawo *et al.* (1999) which was derived as an area average through utilization of satellite data. The evolution of the cliffs and ponds depends on ablation. Sakai *et al.* (2000) argue that the evolution of cliffs and ponds would cause supraglacial debris to fall into the ponds, thus reducing the effective debris thickness. The model should be further improved to include interactions with cliffs and ponds, which are likely to be important.

The debris-free area on the uppermost part has decreased (Seko *et al.*, 1998), so apparently supraglacial debris should have increased on the uppermost part, contrary to the simulation (Fig. 4(b)). This failure of the model could result from neglecting melt-out debris on the upper glacier area and debris supply from lateral slopes. Nakawo *et al.* (1986) estimated that roughly half of the mass of the present supraglacial debris in the ablation area of the Khumbu Glacier was deposited by slope failure of the lateral moraines after the last expansion of the glacier. The present model should be revised to include debris supply from the lateral slopes.

As shown by the dashed curve in Fig. 5, the simulation result is fairly sensitive to the imposed incoming flux from the upper glacier area especially on the upper part. The flux was tuned to fit the observed surface lowering, because the earlier rough estimate by Inoue (1977) led to unreasonably large surface lowering. The tuned flux is about 1.5 times the earlier estimate, which suggests that Inoue (1977) underestimated the area of the upper glacier catchment, that more precipitation falls on the upper area than at Lhajung, and/or that more ice than net accumulation on the upper area flows into the ablation area and consequently the accumulation area is shrinking.

Kodama & Mae (1976) showed that surface flow speed on the ablation area had a seasonal variation, i.e. higher from May to August than the rest of the year. This

seasonal variation should be caused by a variation in basal sliding and/or deformation of the subglacial till layer. Contributions to glacier flow from both of these processes were put together into a variable U_b , which was determined to depend only on location (x) as shown in Fig. 3, ignoring its seasonal and interannual variation. According to previous studies (e.g. Iken & Bindschadler, 1986; Boulton & Hindmarsh, 1987), water pressure at the bed layer should have an important role in both of these processes. Thus, inclusion of subglacial hydraulics could be important for accurate treatment. This defect in the model, however, seems to be minor and does not seriously effect the simulation results as shown by the dotted curve in Fig. 5.

The recent shrinkage of Khumbu Glacier was reasonably simulated in this study. Future projection predicted that stagnant ice in the lowest part would become separated from the main glacier body. This would imply that the Khumbu Glacier could develop a large glacial lake. In order to simulate the significant expansion in the past, e.g. in Little Ice Age, and the following shrinkage of the glacier, inclusion of the accumulation area into the model and long-term climate data would be required.

Acknowledgements This study is based on many contributions by Glaciological Expeditions in Nepal (GEN) activities; cooperation with Department of Hydrology and Meteorology (DHM), Ministry of Science and Technology, His Majesty's Government of Nepal. We would like to thank all members of GEN and the staff of DHM. Special thanks would be expressed to Prof. S. Iwata, Tokyo Metropolitan University, for providing information on topographic surveys in 1978. Grateful thanks also go to Prof. Y. Ageta, Nagoya University; Prof. E. D. Waddington and Dr. H. Conway, University of Washington, for their advice and for developing our numerical model in its formative stage. We would also like to thank Dr A. G. Fountain, Portland State University; Dr K. A. Brugger, University of Minnesota; and another anonymous reviewer for their valuable suggestions. This study was supported by Cooperative Research under the Japan-US Cooperative Science Program from the Japan Society for the Promotion of Science; US National Science Foundation Grant no. INT-9726704 from the National Science Foundation, USA; and a Grant-in-Aid for Scientific Research (no. 09490018) from the Ministry of Education, Science, Sports and Culture, Japanese Government.

REFERENCES

- Ageta, Y. (1983) Characteristics of mass balance of the summer-accumulation type glacier in the Nepal Himalayas (in Japanese with an English abstract). *J. Japan. Soc. Snow Ice (Seppyo)* **45** (2), 81–105.
- Ageta, Y. & Kadota, T. (1992) Predictions of changes of glacier mass balance in the Nepal Himalaya and Tibetan Plateau: a case study of air temperature increase for three glaciers. *Ann. Glaciol.* **16**, 89–94.
- Boulton, G. S. & Hindmarsh, R. C. A. (1987) Sediment deformation beneath glaciers: rheology and geological consequences. *J. Geophys. Res.* **92**, 9059–9082.
- Gades, A., Conway, H., Nererson, N., Naito, N. & Kadota, T. (2000) Radio echo-sounding through supraglacial debris on Lirung and Khumbu Glaciers, Nepal Himalayas. In: *Debris-Covered Glaciers* (ed. by M. Nakawo, C. F. Raymond & A. Fountain) (Proc. Seattle Workshop, September 2000). IAHS Publ. no. 264 (this volume).
- Glaciological Expedition of Nepal (1980) Appendix 1. Glaciological data of the Khumbu Glacier in 1978. *J. Japan. Soc. Snow Ice (Seppyo)* **41**, special issue, 107–110 (with 5 separate sheets).
- Iken, A. & Bindschadler, R. A. (1986) Combined measurements of subglacial water pressure and surface velocity of Findelengletscher, Switzerland: conclusions about drainage system and sliding mechanism. *J. Glaciol.* **32**, 101–119.
- Inoue, J. (1976) Climate of Khumbu Himal. *J. Japan. Soc. Snow Ice (Seppyo)* **38**, special issue, 66–73.

- Inoue, J. (1977) Mass budget of Khumbu Glacier. *J. Japan. Soc. Snow Ice (Seppyo)* **39**, special issue, 15–19.
- Inoue, J. & Yoshida, M. (1980) Ablation and heat exchange over the Khumbu Glacier. *J. Japan. Soc. Snow Ice (Seppyo)* **41**, special issue, 26–33.
- Iwata, S., Watanabe, O. & Fushimi, H. (1980) Surface morphology in the ablation area of the Khumbu Glacier. *J. Japan. Soc. Snow Ice (Seppyo)* **41**, special issue, 9–17.
- Kadota, T. & Ageta, Y. (1992) On the relation between climate and retreat of Glacier AX010 in the Nepal Himalaya from 1978 to 1989. *Bull. Glacier Res.* **10**, 1–10.
- Kadota, T., Seko, K., Aoki, T., Iwata, S. & Yamaguchi, S. (2000) Shrinkage of the Khumbu Glacier, east Nepal from 1978 to 1995. In: *Debris-Covered Glaciers* (ed. by M. Nakawo, C. F. Raymond & A. Fountain) (Proc. Seattle Workshop, September 2000). IAHS Publ. no. 264 (this volume).
- Kodama, H. & Mae, S. (1976) The flow of glaciers in the Khumbu region. *J. Japan. Soc. Snow Ice (Seppyo)* **38**, special issue, 31–36.
- Lam, J. K.-W. & Dowdeswell, J. A. (1996) An adaptive-grid finite-volume model of glacier-terminus fluctuations. *Ann. Glaciol.* **23**, 86–93.
- Mattson, L. E., Gardner, J. S. & Young, G. J. (1993) Ablation on debris covered glaciers: an example from the Rakhiot Glacier, Punjab, Himalaya. In: *Snow and Glacier Hydrology* (ed. by G. J. Young) (Proc. Kathmandu Symp., November 1992), 289–296. IAHS Publ. no. 218.
- Nakawo, M., Iwata, S., Watanabe, O. & Yoshida, M. (1986) Processes which distribute supraglacial debris on the Khumbu Glacier, Nepal Himalaya. *Ann. Glaciol.* **8**, 129–131.
- Nakawo, M., Yabuki, H. & Sakai, A. (1999) Characteristics of Khumbu Glacier, Nepal Himalaya: recent change in the debris-covered area. *Ann. Glaciol.* **28**, 118–122.
- National Geographic Society (1988) *Mount Everest*. National Geographic Society, Washington, DC.
- Nye, J. F. (1965) The flow of a glacier in a channel of rectangular, elliptic or parabolic cross-section. *J. Glaciol.* **5**, 661–690.
- Østrem, G. (1959) Ice melting under a thin layer of moraine, and the existence of ice cores in moraine ridges. *Geogr. Ann.* **41**, 228–230.
- Patankar, S. V. (1980) *Numerical Heat Transfer and Fluid Flow*. Hemisphere, New York.
- Paterson, W. S. B. (1994) *The Physics of Glaciers*, 3rd edn. Elsevier, Oxford.
- Sakai, A., Takeuchi, N., Fujita, K. & Nakawo, M. (2000) Role of supraglacial ponds in the ablation process of a debris-covered glacier in the Nepal Himalayas. In: *Debris-Covered Glaciers* (ed. by M. Nakawo, C. F. Raymond & A. Fountain) (Proc. Seattle Workshop, September 2000). IAHS Publ. no. 264 (this volume).
- Seko, K., Yabuki, H., Nakawo, M., Sakai, A., Kadota, T. & Yamada Y. (1998) Changing surface of Khumbu Glacier, Nepal Himalayas revealed by SPOT images. *Bull. Glacier Res.* **16**, 33–41.
- Watanabe, O., Fushimi, H., Inoue, J., Iwata, S., Ikegami, K., Tanaka, Y., Yoshida, M. & Upadhyay, B. P. (1980) Outline of debris cover project in Khumbu Glacier. *J. Japan. Soc. Snow Ice (Seppyo)* **41**, special issue, 5–8.
- Watanabe, O., Iwata, S. & Fushimi, H. (1986) Topographic characteristics in the ablation area of the Khumbu Glacier, Nepal Himalaya. *Ann. Glaciol.* **8**, 177–180.